

# Large tunable delays using parametric mixing and phase conjugation in Si nanowaveguides

Yoshitomo Okawachi<sup>1</sup>, Mark A. Foster<sup>1</sup>, Xianpei Chen<sup>1</sup>,  
Amy C. Turner-Foster<sup>2</sup>, Reza Salem<sup>1</sup>, Michal Lipson<sup>2</sup>,  
Chris Xu<sup>1</sup>, and Alexander L. Gaeta<sup>1</sup>

<sup>1</sup>*School of Applied and Engineering Physics, Cornell University, Ithaca, NY 14853*

<sup>2</sup>*School of Electrical and Computer Engineering, Cornell University, Ithaca, NY 14853*

[a.gaeta@cornell.edu](mailto:a.gaeta@cornell.edu)

**Abstract:** We demonstrate a technique for generating large, all-optical delays while simultaneously minimizing pulse distortion by using temporal phase conjugation via four-wave mixing in Si nanowaveguides. Using this scheme, we achieve continuously tunable delays over a range of 243 ns for 10 Gb/s NRZ data.

© 2008 Optical Society of America

**OCIS codes:** (190.4380) Nonlinear optics, four-wave mixing; (190.4390) Nonlinear optics, integrated optics

---

## References and links

1. M. K. Dhodhi, S. Tariq, and K. A. Saleh, "Bottlenecks in next generation DWDM-based optical networks," *Comput. Commun.* **24**, 1726–1733 (2001).
2. M. Saruwatari, "All-optical signal processing for Terabit/Second Optical Transmission," *IEEE J. Sel. Top. Quantum Electron.* **6**, 1363–1374 (2000).
3. S. J. B. Yoo, "Optical packet and burst switching technologies for the future photonic internet," *J. Lightwave Technol.* **24**, 4468–4492 (2006).
4. E. Choi, J. H. Na, Y. Ryu, G. Mudhana, and B. H. Lee, "All-fiber variable optical delay line for applications in optical coherence tomography: feasibility study for a novel delay line," *Opt. Express* **13**, 1334–1345 (2005).
5. J. L. Corral, J. Marti, J. M. Fuster, and R. I. Laming, "True time-delay scheme for feeding optically controlled phased-array antennas using chirped-fiber gratings," *Photon. Technol. Lett.* **9**, 1529–1531 (1997).
6. G. N. Pearson, K. D. Ridley, and D. V. Willetts, "Chirp-pulse-compression three dimensional lidar imager with fiber optics," *Appl. Opt.* **44**, 257–265 (2005).
7. Y. Han and B. Jalali, "Photonic time-stretched analog-to-digital converter: Fundamental concepts and practical considerations," *J. Lightwave Technol.* **21**, 3085–3103 (2003).
8. R. Ramaswami and K. N. Sivarajan, *Optical Networks: A Practical Perspective* (Morgan Kaufmann, 2002).
9. R. W. Boyd and D. J. Gauthier, "'Slow' and 'fast' light," *Progress in Optics* **43**, edited by E. Wolf (Elsevier, Amsterdam, 2002), Chap. 6, p. 497–530.
10. R. W. Boyd, D. J. Gauthier, and A. L. Gaeta, "Applications of slow light in telecommunications," *Opt. Photon. News* **17**, 18–22 (2006).
11. M. Burzio, P. Cinato, R. Finotti, P. Gambini, M. Puleo, E. Vezzoni, and L. Zucchelli, "Optical cell synchronization in an ATM optical switch," in *Proc. ECOC '94, Florence, Italy*, **2**, 581–584 (1994).
12. L. Zucchelli, M. Burzio, and P. Gambini, "New solutions for optical packet delineation and synchronization in optical packet switched networks," in *Proc. ECOC '96, Oslo, Norway*, **3**, 301–304 (1996).
13. K. Shimizu, G. Kalogerakis, K. Wong, M. Marhic, and L. Kazovsky, "Timing jitter and amplitude noise reduction by a chirped pulsed-pump fiber OPA," in *Proc. OFC '03, Anaheim, USA*, **1**, 197–198 (2003).
14. J. van Howe and C. Xu, "Ultrafast optical delay line using soliton propagation between a time-prism pair," *Opt. Express* **13**, 1138–1143 (2005).
15. S. Oda and A. Maruta, "All-optical tunable delay line based on soliton self-frequency shift and filtering broadened spectrum due to self-phase modulation," *Opt. Express* **14**, 7895–7902 (2006).

16. Y. Wang, C. Yu, L. Yan, A. E. Willner, R. Roussev, C. Langrock, M. M. Fejer, J. E. Sharping, and A. E. Gaeta, "44-ns continuously tunable dispersionless optical delay element using a PPLN waveguide with two-pump configuration, DCF, and a dispersion compensator," *Photon. Technol. Lett.* **19**, 861–863 (2007).
17. L. C. Christen, I. Fazal, O. Yilmaz, X. Wu, S. R. Nuccio, A. E. Willner, C. Langrock, and M. Fejer, "Tunable 105-ns optical delay for 80-Gb/s RZ-DQPSK, 40-Gbit/s RZ-DPSK, and 40-Gbit/s RZ-OOK signals using wavelength conversion and chromatic dispersion," *Optical Fiber Communication Conference*, paper OTuD1 (2008).
18. J. E. Sharping, Y. Okawachi, J. van Howe, C. Xu, Y. Wang, A. E. Willner, and A. L. Gaeta, "All-optical, wavelength and bandwidth preserving, pulse delay based on parametric wavelength conversion and dispersion," *Opt. Express* **13**, 7872–7877 (2005).
19. J. Ren, N. Alic, E. Myslivets, R. E. Saperstein, C. J. McKinstrie, R. M. Jopson, A. H. Gnauck, P. A. Andrekson, and S. Radic, "12.47 ns continuously-tunable two-pump parametric delay," *European Conference on Optical Communications*, paper Th4.4.3 (2006).
20. M. P. Fok and C. Shu, "Tunable optical delay using four-wave mixing in a 35-cm highly nonlinear bismuth-oxide fiber and group velocity dispersion," *J. Lightwave Technol.* **26**, 499–504 (2008).
21. Y. Okawachi, J. E. Sharping, C. Xu, and A. L. Gaeta, "Large tunable optical delays via self-phase modulation and dispersion," *Opt. Express* **14**, 12022–12027 (2006).
22. Z. Hu and D. J. Blumenthal, "SPM-based 2R regenerative 10Gbps optically linearly controlled delay line with Ops to 170ps tuning range," in *Proc. OFC '07, Anaheim, USA, OME4* (2007).
23. Y. Okawachi, R. Salem, and A. L. Gaeta, "Continuous tunable delays at 10-Gb/s data rates using self-phase modulation and dispersion," *J. Lightwave Technol.* **25**, 3710–3715 (2007).
24. M. A. Foster, A. C. Turner, R. Salem, M. Lipson, and A. L. Gaeta, "Broad-band continuous-wave parametric wavelength conversion in silicon nanowaveguides," *Opt. Express* **15**, 12,949–12,958 (2007).
25. A. C. Turner, C. Manolatou, B. S. Schmidt, M. Lipson, M. A. Foster, J. E. Sharping, and A. L. Gaeta, "Tailored anomalous group-velocity dispersion in silicon channel waveguides," *Opt. Express* **14**, 4357–4362 (2006).
26. M. A. Foster, A. C. Turner, J. E. Sharping, B. S. Schmidt, M. Lipson, and A. L. Gaeta, "Broad-band optical parametric gain on a silicon photonic chip," *Nature* **441**, 960–963 (2006).
27. A. Yariv, D. Fekete, and D. M. Pepper, "Compensation for channel dispersion by nonlinear optical phase conjugation," *Opt. Lett.* **4**, 52–54 (1979).
28. S. Ayotte, S. Xu, H. Rong, O. Cohen, and M. J. Paniccia, "Dispersion compensation by optical phase conjugation in silicon waveguide," *Electron. Lett.* **43**, 1037–1039 (2007).
29. G. P. Agrawal, *Nonlinear Fiber Optics* (Academic Press, Boston, 1989).
30. M. Tsang and D. Psaltis, "Dispersion and nonlinearity compensation by spectral phase conjugation," *Opt. Lett.* **28**, 1558–1560 (2003).
31. G. P. Agrawal, *Fiber-Optic Communication Systems* (Wiley Interscience, New York, 2002).
32. M. A. Foster, A. C. Turner, R. Salem, D. F. Geraghty, M. Lipson, and A. L. Gaeta (in preparation).

---

## 1. Introduction

Communication networks require components that have the capability of buffering or delaying information. In ultra-high speed communications, where information is encoded in pulses, optical/electronic conversion of information is a bottleneck for increasing the data transmission rate [1]. While information is transmitted using optical fibers in current communication networks, components for data processing, such as routing and switching, use electronics based on CMOS technology. As the data rate increases and device size decreases, it is becoming more difficult for the industry to follow Moore's law. One solution to this electronic bottleneck problem is the development of an all-optical network [2]. All-optical components will eliminate the bandwidth limitation due to optical/electronic signal conversion and reduce the noise and errors due to the conversion. Optical delay lines have already been implemented in communication systems. However, these delay lines were constructed by combining a series of fixed delay lines with different amounts of delay in parallel to generate discrete delays [3]. Many communication applications require fine tuning of the delay, and these discrete delay lines will not have the granularity that is necessary as the data rates increase. Specific applications for tunable optical delay lines in communication systems include network buffering, data synchronization, and time-division multiplexing. The development of tunable all-optical delay lines is also important for applications other than telecommunication, including optical coherence tomography [4], optical control of phased array antennas for radio frequency communication [5], light detection and sensing (LIDAR) [6], optical sampling [7], and pattern correlation [8]. The method

that has received considerable interest for generating tunable delays uses the concept of slow light, which takes advantage of the rapidly-varying refractive index that accompanies an optical resonance [9]. However, the maximum delay that can be generated in practical slow-light delay lines has been limited to a few pulse widths [10].

An alternative technique for generating tunable delays is using wavelength conversion and dispersion. The conversion-dispersion delay scheme takes advantage of the group-velocity dispersion (GVD) in an optical fiber for generating a wavelength-dependent optical delay [11, 12, 13, 14]. The center wavelength of the input signal is shifted and injected into a medium with a large GVD, which yields a delay with respect to the initial, unshifted pulse. A second wavelength converter can then be used to return the signal wavelength to the original wavelength. The total delay is simply a product of the GVD parameter  $D$ , the length of the dispersive fiber  $L_d$ , and the wavelength shift  $\Delta\lambda$ . Thus to achieve large delays using this scheme, it is necessary to produce a large wavelength shift and/or large a GVD. Several conversion-dispersion delay schemes have been demonstrated, including soliton self-frequency shift [15],  $\chi^{(2)}$  parametric mixing [16, 17], four-wave mixing [18, 19, 20], and self-phase modulation [21, 22, 23].

Recently, wavelength conversion over large bandwidths has been demonstrated in silicon waveguides [24]. The silicon-on-insulator (SOI) platform is in many ways ideal for nonlinear interactions due to the high index contrast between the silicon core and silica cladding, which allows for strong optical confinement and large effective optical nonlinearities, since the nonlinear coefficient is 200 times larger in silicon than in silica glass. Furthermore, the dispersion in the silicon waveguides can be tailored by controlling the size and shape of the waveguides, and anomalous dispersion can be produced within a small range of waveguide dimensions [25]. Foster *et al.* [26] demonstrated FWM gain of 5.2 dB in silicon waveguides using a pulsed pump. Recently, the FWM bandwidths have been extended to well over 100 nm in silicon waveguides [24], which can be attributed to the short interaction length and dispersion tailoring [25]. This broad bandwidth allows for much larger delays as compared to the previous demonstration of the FWM conversion-dispersion scheme in an optical fiber [18]. Another advantage of the silicon platform is that a cw pump can be used without phase modulation since the silicon waveguides do not exhibit stimulated Brillouin scattering.

The other method for extending the maximum achievable delay in the conversion-dispersion scheme is by increasing the length of the dispersive fiber used in the delay stage. However, due to dispersive broadening of the pulse, a limit exists on the maximum amount of dispersion that can be used without additional compensating elements. Dispersion compensators, such as chirped fiber Bragg gratings, can be implemented to extend the allowable GVD in the dispersive fiber [16]. In this case, the GVD in the dispersion compensator must be tailored such that it has the same magnitude and the opposite sign as the GVD in the dispersive fiber. In this paper we discuss a simple technique that overcomes the GVD-induced pulse broadening by using the inherent temporal phase conjugation associated with FWM, which allows us to further extend the maximum achievable delay. A delay scheme that utilizes phase conjugation has been previously demonstrated using a two-pump FWM scheme, in which delays of 12.5 ns for a 10 Gb/s signal were generated [19]. The delay scheme consists of three stages, the first is a dispersive fiber with dispersion  $+D$ , the second is a FWM wavelength conversion and phase conjugation stage, and the third is a dispersive fiber with dispersion  $+D$  (Fig. 1). Since the sign and the magnitude of the dispersion need to be the same in the first and third stages, we incorporate a scheme in which the same dispersive fiber is used for the dispersion compensation and the dispersive delay. Using this technique, we demonstrate a tuning range of 243 ns for a 10 Gb/s NRZ input signal with minimal pulse distortion.

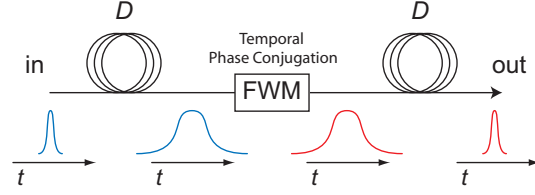


Fig. 1. Delay generator using wavelength conversion and temporal phase conjugation via FWM and two dispersion links. The FWM stage acts both as a wavelength converter and a phase conjugator.

## 2. Theory

Temporal phase conjugation (TPC) results in the generated field being the complex conjugate of the input field, which results in phase reversal. FWM is a standard technique used to perform TPC [27, 28] in which the signal and idler fields are related through the complex conjugate [29].

The equation describing propagation through the first dispersive fiber can be written as follows, including contributions from third-order dispersion (TOD) and assuming no nonlinearity [29],

$$\frac{\partial A}{\partial z} + i\frac{\beta_2}{2}\frac{\partial^2 A}{\partial T^2} - \frac{\beta_3}{6}\frac{\partial^3 A}{\partial T^3} = 0. \quad (1)$$

If the field now undergoes TPC, the propagation through the second dispersive fiber can be written as,

$$\frac{\partial A^*}{\partial z} - i\frac{\beta_2}{2}\frac{\partial^2 A^*}{\partial T^2} - \frac{\beta_3}{6}\frac{\partial^3 A^*}{\partial T^3} = 0. \quad (2)$$

Comparing Eqs. (1) and (2), the conjugated field experience a second-order dispersion of the opposite sign. Thus, TPC allows cancellation between the GVD of the first fiber and the second fiber, making it equivalent to operating in the zero-GVD regime. However, this technique only compensates for even-order dispersion terms [30]. In addition, there exists residual dispersion from the fact that the wavelength is shifted. Thus, the maximum achievable delay is limited by this residual dispersion and the TOD.

The maximum allowable GVD and delay are determined by evaluating the broadening factor due to TOD and residual dispersion from the wavelength shift [31]. Assuming a Gaussian pulse profile, the broadening factor can be expressed as,

$$\frac{\sigma^2}{\sigma_0^2} = 1 + \left(\frac{\beta_{2R}L}{4\sigma_0^2}\right)^2 + \left(\frac{\beta_3L}{4\sqrt{2}\sigma_0^3}\right)^2, \quad (3)$$

where  $\sigma$  is the root-mean-square (RMS) pulsewidth after the two fibers,  $\sigma_0$  is the RMS pulsewidth of the input,  $L$  is the combined length of the first and second dispersive fibers.  $\beta_{2R}$  is the residual second-order dispersion, which is the difference in the second-order dispersion for a 70 nm wavelength shift. The RMS pulsewidth  $\sigma_0$  can be expressed in terms of the FWHM pulsewidth as,

$$\sigma_0 = \frac{T_{FWHM}}{2(2\ln 2)^{1/2}}. \quad (4)$$

The condition used to determine the maximum allowable broadening is

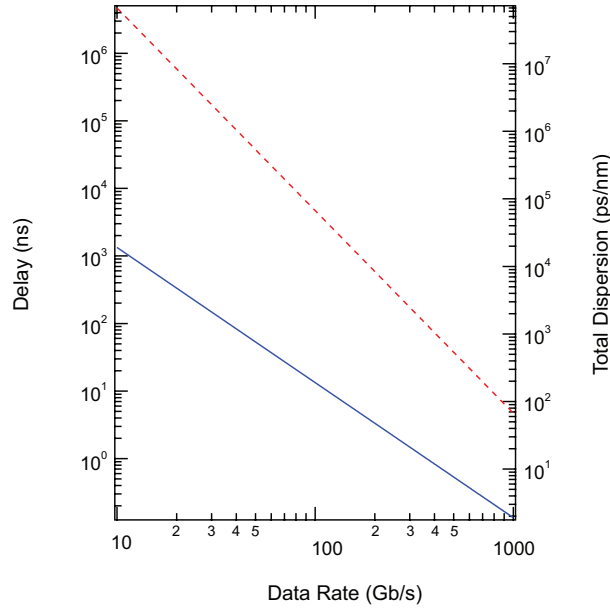


Fig. 2. Maximum delay (left axis) and the magnitude of the allowable dispersion (right axis) as a function of input data rate. We assume RZ pulses with a 33% fill-factor as our input and a wavelength conversion bandwidth of 70 nm. The dashed red line shows the achievable delay if TOD compensation is not performed, and the solid blue line shows achievable delay without residual second-order dispersion and TOD compensation.

$$4B\sigma \leq 1, \quad (5)$$

where  $B$  is the bit rate. This condition is set so that 95% of the pulse energy remains within the bit slot [31]. We use a relative dispersion slope (RDS), which is the ratio between the dispersion slope and the dispersion parameter, that is approximately a factor of 10 smaller than that of standard SMF fiber. A dispersive fiber with a larger RDS will significantly reduce the achievable delay, especially at the higher data rates. For example, using an RDS value of standard SMF will reduce the delay achievable by an order of magnitude at 10 Gb/s data rates. Figure 2 shows the maximum total GVD allowed in the dispersive fiber and the corresponding maximum delay that can be achieved for various input data rates when phase conjugation is used. We assume that the signal and the pump in the FWM process are all within the C-band of the telecommunications window, and the conversion occurs across both the C- and L-bands, which corresponds to a maximum wavelength conversion of 70 nm. The solid blue line represents the delay that can be achieved without compensation of TOD and the residual second-order dispersion due to the wavelength shift. One possible means of compensating for the residual dispersion is the use of a tunable dispersion compensator at the input. The dashed red line represents the delay that can be achieved without compensation of TOD. We show theoretically that the lower the data rate, the larger the amount of GVD that can be used in the dispersive fiber stage. However, in practice, there exists an upper limit on the length of fiber due to losses and the latency for generating the delay due to the long distances through which the pulses need to propagate.

### 3. Experiment

The experimental setup is shown in Fig. 3(a). The signal centered at 1535 nm is modulated using a pattern generator and a Mach-Zhender modulator to generate NRZ pulses at 10 Gb/s. The pulses are sent through a circulator into a length of dispersion compensating fiber (DCF). For our initial experiment, we use a DCF with a total dispersion of -2600 ps/nm. The signal is then sent through the second circulator, amplified using a C-band EDFA, and combined with a cw pump. The pump power is 100-200 mW and the signal power is kept approximately 5 dB below the pump power for optimal wavelength conversion. The amplified signal and pump are coupled into a 1.48 cm long silicon waveguide, with a cross section of 300 nm by 750 nm, for FWM wavelength conversion and phase conjugation [Fig. 3(b)]. The output is amplified using C- and L-band EDFA preamplifiers, sequentially and sent back into the second circulator, through the same DCF, and into the first circulator. Finally, the output is filtered using a tunable bandpass filter and measured using a sampling oscilloscope. If a fixed wavelength operation is necessary, a second wavelength conversion stage can be implemented at the output to return to the input signal wavelength [18]. The major advantage of this configuration is that the same dispersive fiber is used for both dispersive delay and dispersion compensation, which eliminates an extra component and the need for dispersion matching.

Figure 4 shows a plot of delay as a function of the converted idler wavelength. The idler wavelength is tuned over a total range of 39 nm, which covers parts of the C- and L-band of the telecom window, and we achieve a maximum tuning range of 100 ns, which is limited by the C-band EDFA's that are used for the pump. The maximum wavelength to which the pump can be tuned is 1565 nm. The decrease in pump amplification beyond this point reduces the FWM conversion efficiency. The idler wavelength could not be tuned over the entire C-band due to absorption in the L-band EDFA for wavelengths below approximately 1550 nm.

We further extend the delay by using DCF with a total dispersion of -3600 ps/nm. To achieve 0 dB transmission loss through the DCF, we use Raman pumps from both directions to amplify

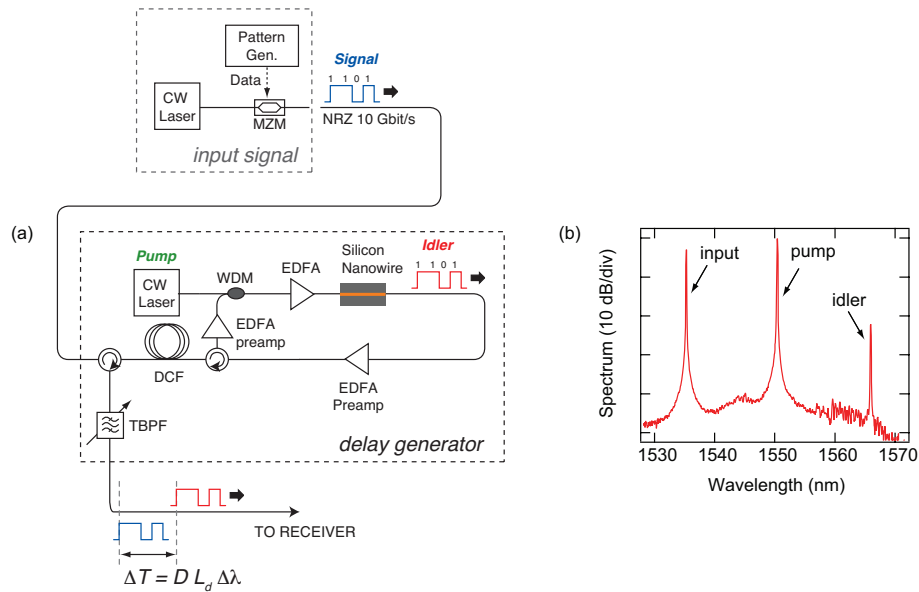


Fig. 3. (a) Experimental setup for delay scheme based on wavelength conversion and phase conjugation. (b) Four-wave mixing spectrum from the silicon waveguide.

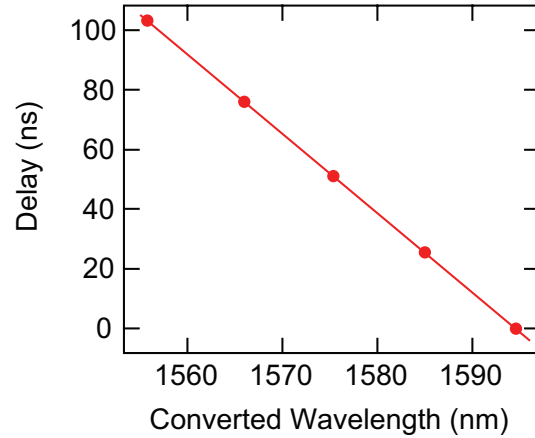


Fig. 4. Measured delay as a function of the converted wavelength using a total dispersion of  $-2600$  ps/nm for the set-up shown in Fig. 4(a).

the transmitted signal. The gain we achieve with the Raman pumps allows us to remove the C- and L-band EDFA preamplifiers, which permits a larger range of wavelength conversion. Figure 5 shows the delay traces for three different converted idler wavelengths, and Fig. 6 shows the delay as a function of the converted idler wavelength. The tuning range of the idler wavelength is now extended to 66 nm. Using this scheme, we achieve a maximum tuning range of 243 ns.

Figure 7 shows the eye diagrams measured at various points in the delay generator. Figure 7(a) shows the eye diagram of the input signal, and 7(b) shows the eye diagram immediately after the first pass through the DCF with a total dispersion of  $-3600$  ps/nm. It is clear from the plot that the signal undergoes significant pulse broadening and that the eye is closed. Figure 7(c) shows the eye diagram at the output of the delay generator. As a result of the FWM phase conjugation, the dispersive broadening of the pulses is minimized. The achievable delay is currently

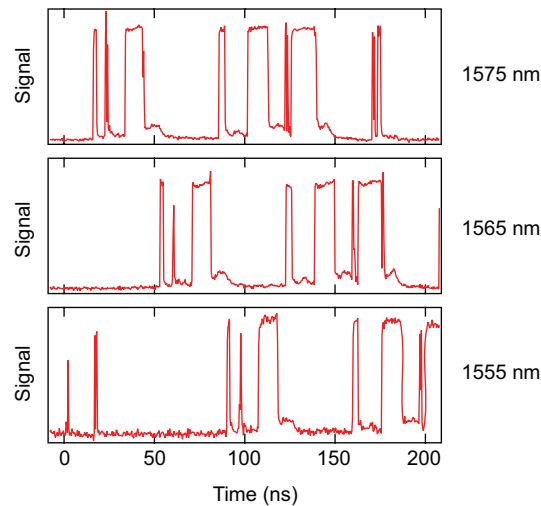


Fig. 5. Experimental results for the delay scheme based on wavelength conversion and phase conjugation. Traces represent idler wavelengths of 1555 nm, 1565 nm, and 1575 nm.

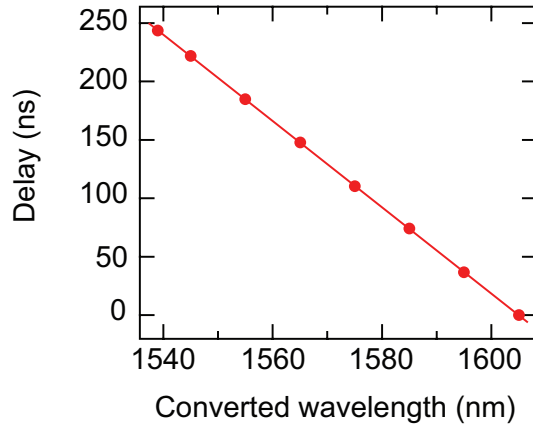


Fig. 6. Measured delay as a function of the converted wavelength using a DCF with a total dispersion of  $-3600$  ps/nm and implementing the double-pass scheme with FWM phase conjugation.

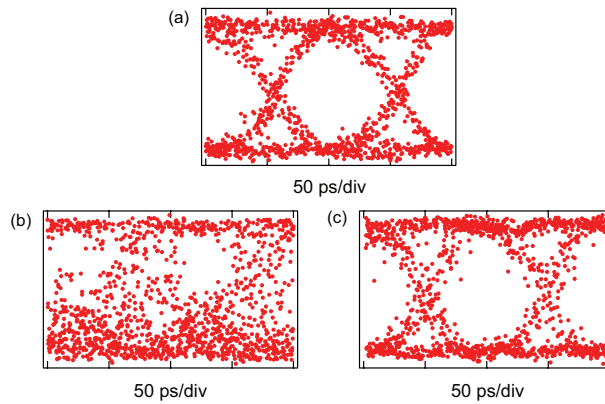


Fig. 7. Eye diagrams of (a) the input, (b) after the first DCF, and (c) the output through the delay generator.

limited primarily by losses in the silicon waveguide. The combination of the linear loss and the nonlinear loss, due to two-photon absorption and free-carrier absorption, limits the efficiency of the FWM process in the silicon waveguides. As a result of these losses, optical amplifiers are required at the output to boost the power of the generated idler. This limits the FWM bandwidth that can be utilized since the optical amplifiers have a limited gain bandwidth.

#### 4. Conclusion

In conclusion, we have demonstrated tunable delays as large as 243 ns for 10 Gb/s NRZ signals using FWM phase conjugation and dispersion, which corresponds to a delay-bandwidth product of 2430. Temporal phase conjugation allows for use of large GVD without pre- or post-compensation of the pulse broadening due to second-order dispersion. Broadband FWM over 500-nm bandwidths have been recently demonstrated [32]. Thus, by reducing the losses in the silicon waveguides and by improving the conversion efficiency, the need for optical amplifiers will be eliminated, and the entire FWM conversion bandwidth can be utilized, which will enable extension of the delays to  $1 \mu\text{s}$ .

## **Acknowledgments**

We gratefully acknowledge support from the Center for Nanoscale Systems, supported by the NSF and the DARPA MTO POPS Program. Y.O., M.A.F., R.S., and A.L.G. gratefully acknowledge support from the DARPA DSO Slow-Light Program.